Towards improving the antibiotic elimination capacity of UiO-66 from contaminated water

Supporting Information

Sara Rojas,[a,b] Ana Torres,[a] Víctor Dato,[a] Fabrice Salles,[c] David Ávila,[d] Jessica García-González,[e] Patricia Horcajada[a,]*

[a] Advanced Porous Materials Unit, IMDEA Energy. Av. Ramón de la Sagra 3, 28935 Móstoles-Madrid, Spain.

[b] Department of Inorganic Chemistry, Faculty of Science, University of Granada, 18071 Granada, Spain.

[c] ICGM, Univ. Montpellier, CNRS, ENSCM, Montpellier, France.

[d] Department of Inorganic Chemistry, Chemical Sciences Faculty, Complutense University of Madrid, 28040 Madrid, Spain.

[e] Department of Nursing, Faculty of Health and Social Sciences, University of Murcia. Campus de Lorca, 30800 Murcia, Spain.

* patricia.horcajada@imdea.org

Table on Contents

S1. Photocatalytic degradation of sulfamethazine (SMT) in water using UiO-66

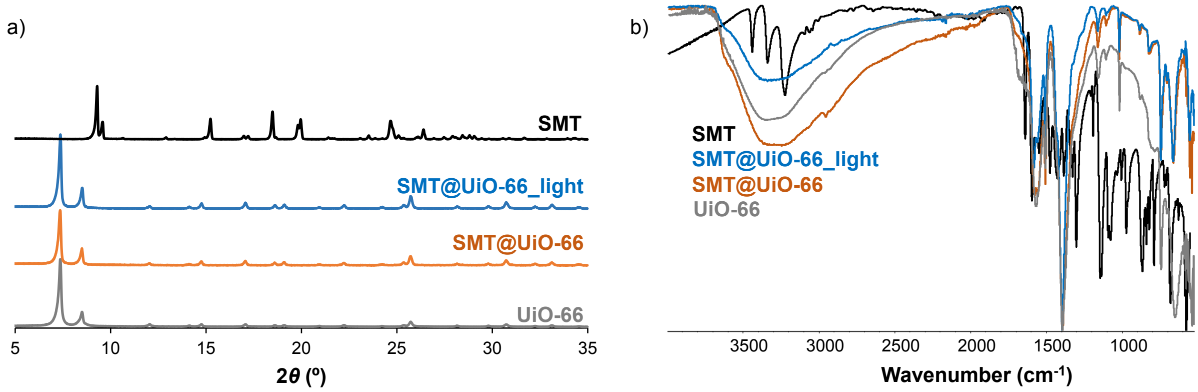

Figure S1. a) X-ray powder diffraction (XRPD) patterns, and b) Fourier transform infrared (FTIR) spectra of the UiO-66 before (grey), and after being suspended in a SMT tap aqueous solution for 24 h under UV-vis irradiation or darkness (blue and orange, respectively; denoted as SMT@UiO-66_light and SMT@UiO-66). XRPD pattern and FTIR spectrum of SMT were added for comparison.

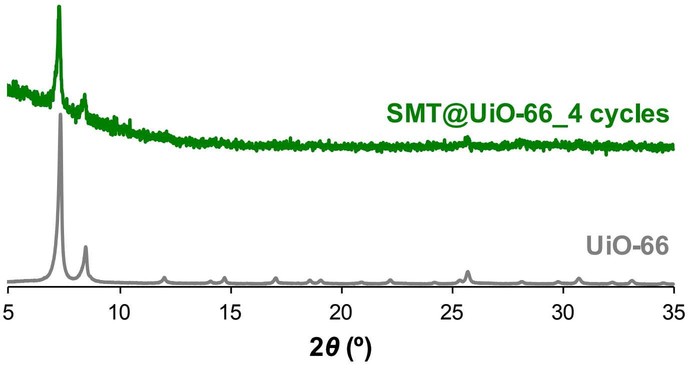

Figure S2. XRPD patterns of the UiO-66 before (grey) and after 4 cycles of SMT photodegradation (green).

S2. NanoUiO-66-X characterization

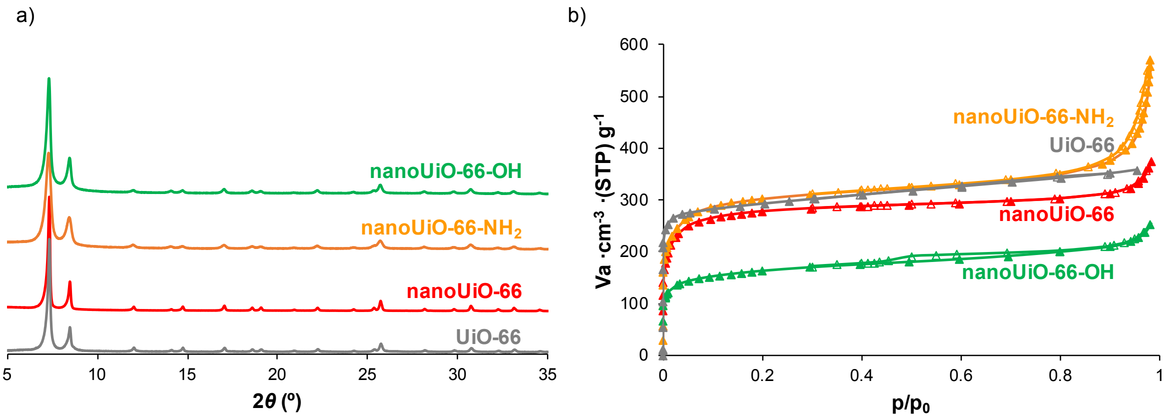

Figure S3. a) XRPD patterns, and b) N_2 sorption isotherms of the nanoUiO-X series (X = H, NH_2, and OH) and UiO-66. Solid and empty symbols indicate adsorption and desorption branches, respectively.

Table S1. Textural properties of MOFs. External surface area was calculated by t-plot method (p/p_0 from 0.3 to 0.6).

	S_{BET} ($m^2 \cdot g^{-1}$)	**Pore volume ($cm^3 \cdot g^{-1}$)**	**External Surface Area ($m^2 \cdot g^{-1}$)**
UiO-66	1230	0.31	190
nanoUiO-66	1010	0.31	290
nanoUiO-66-NH$_2$	1130	0.34	290
nanoUiO-66-OH	600	0.16	210

Table S2. Particle size (nm) and ζ-potential (mV) estimated using scanning and transmission electron microscopy (SEM/TEM) images, and DLS measurements (including the PDI) of UiO-66 and nanoUiO-X series (X = H, NH_2, and OH) in 1 minute-aged suspension in water. The pH value of all these suspensions were found to be *ca.* 6.

	Size SEM/TEM (nm)	**Size DLS (nm) (PDI)**	**ζ-potential (mV)**
UiO-66	672 ± 181	ND	+ 30 ± 1-
nanoUiO-66-H	81 ± 27	460 ± 30 (0.6)	- 17 ± 1
nanoUiO-66-NH$_2$	38 ± 17	162 ± 4 (0.5)	+ 21 ± 3
nanoUiO-66-OH	118 ± 68	673 ± 142 (0.8)	- 22 ± 1

ND: Not determined

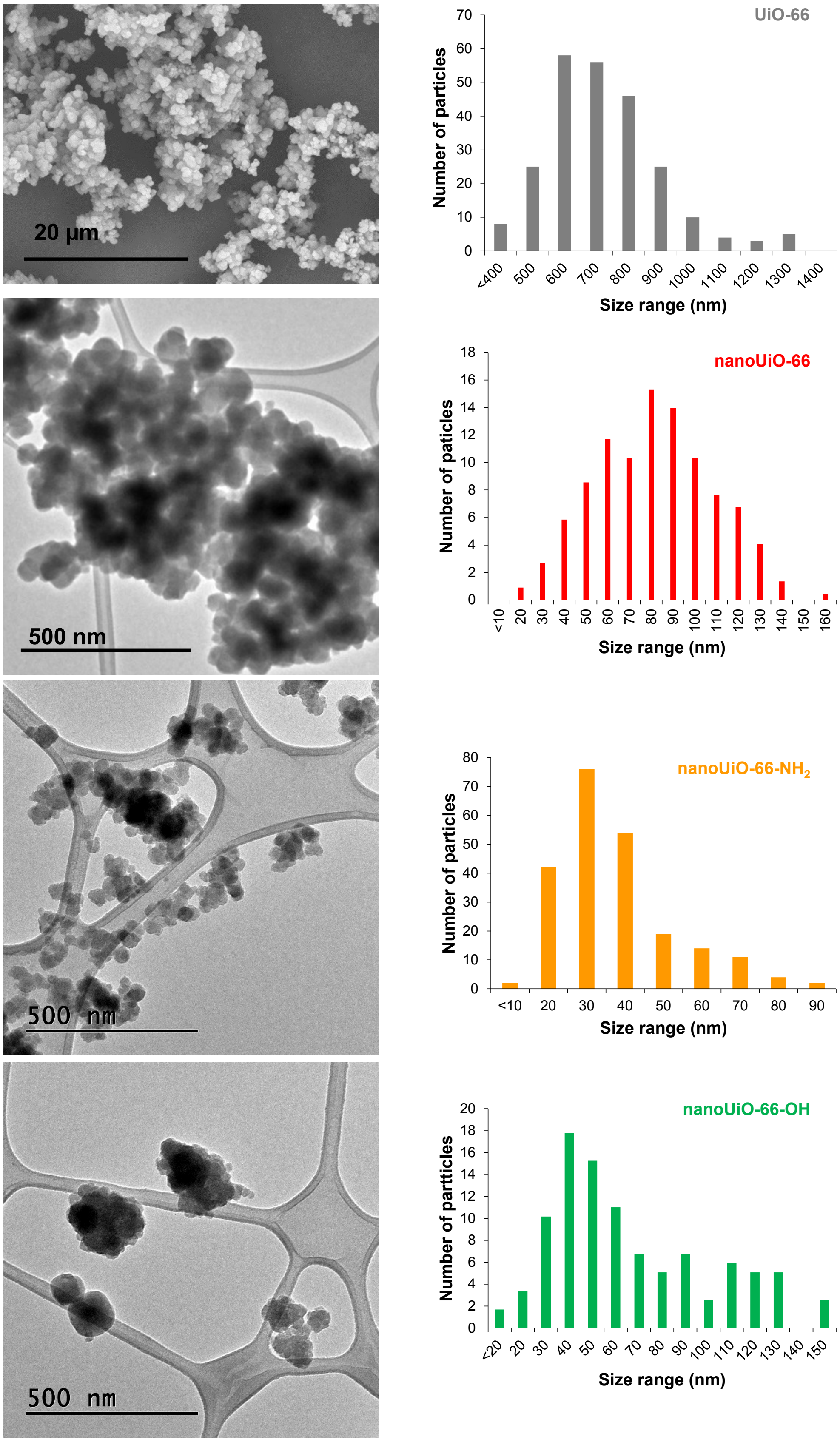

Figure S4. SEM and TEM images and particle size distribution for UiO-66, and nanoUiO-66-X (X = H, NH_2, and OH).

S3. Adsorption and/or photodegradation of SMT in water using nanoUiO-66-X

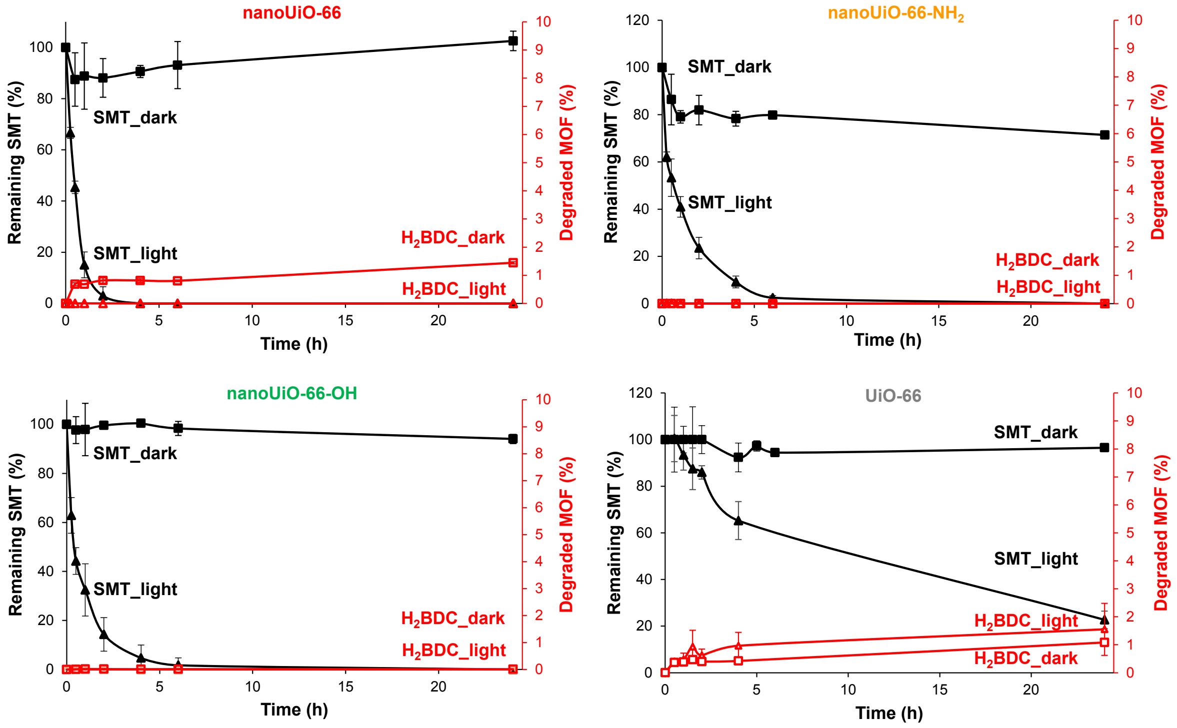

Figure S5. Effect of time on the adsorption and photodegradation of SMT (black squares and triangles respectively, left y axis) using nanoUiO-66-X (X = H, NH_2, and OH). MOFs degradation over time is also represented (in red using squares and triangles respectively, right y axis).

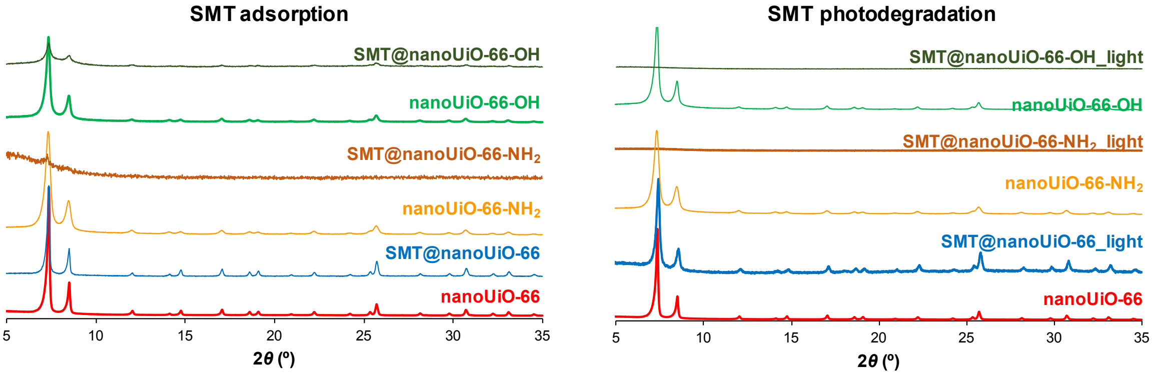

Figure S6. XRPD patterns of nanoUiO-66-H (H = H, NH_2, and OH) before and after being suspended in a SMT tap aqueous solution under dark and Vis irradiation for 24 h (denoted as SMT@nanoUiO-66-X and SMT@nanoUiO-66-X_light, respectively).

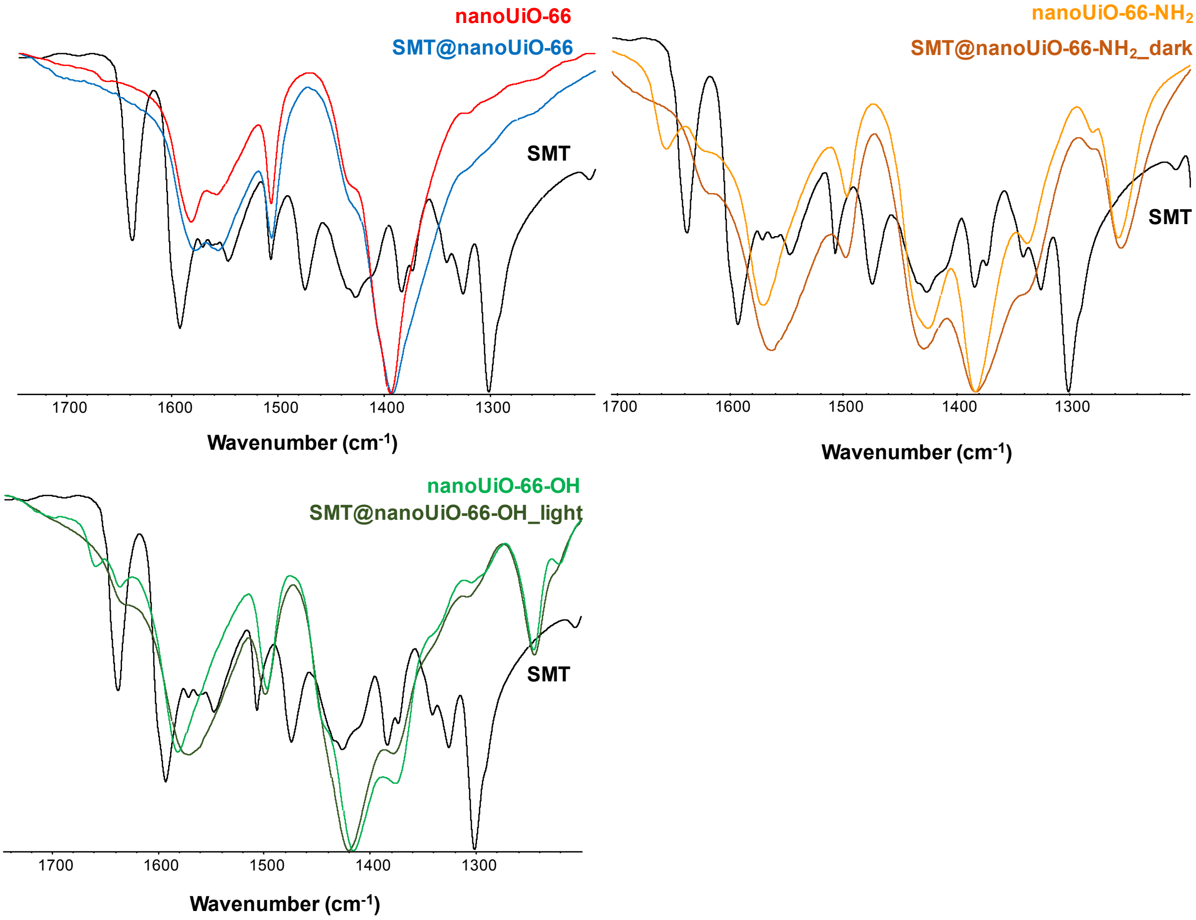

Figure S7. FTIR spectra of the nanoUiO-66-X (X = H, NH$_2$, and OH), and their corresponding SMT (SMT@nanoUiO-66-X) loaded materials. The spectrum of the free SMT has been included for comparison.

Computational section

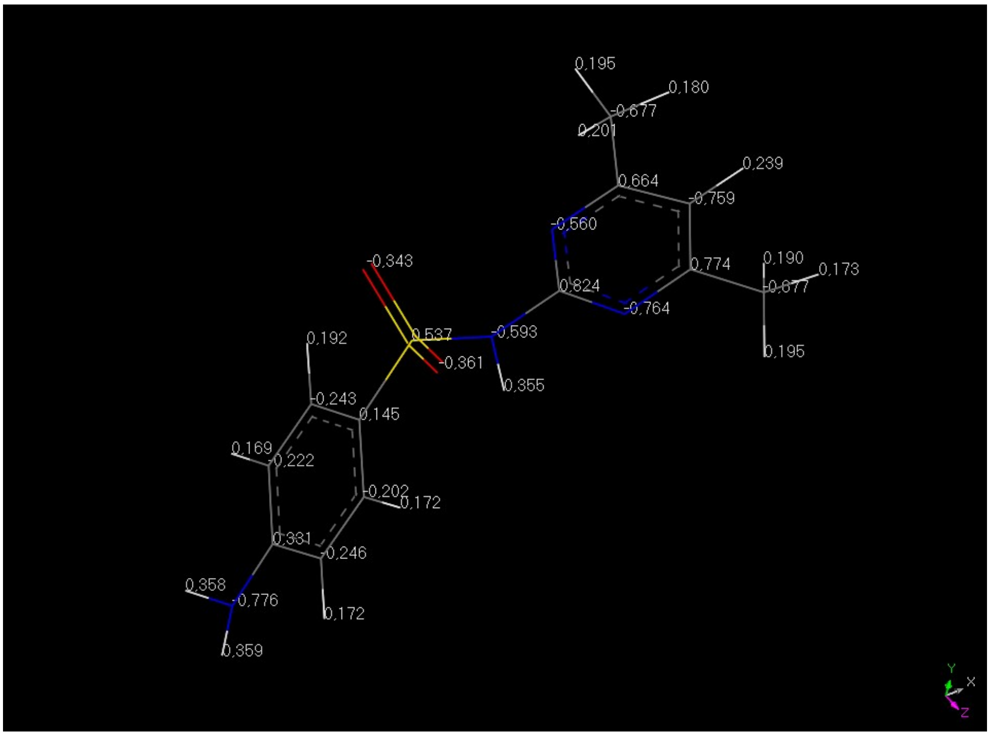

Figure S8. Partial charges of the SMT molecule obtained by DFT calculations and implemented in Monte Carlo simulations.

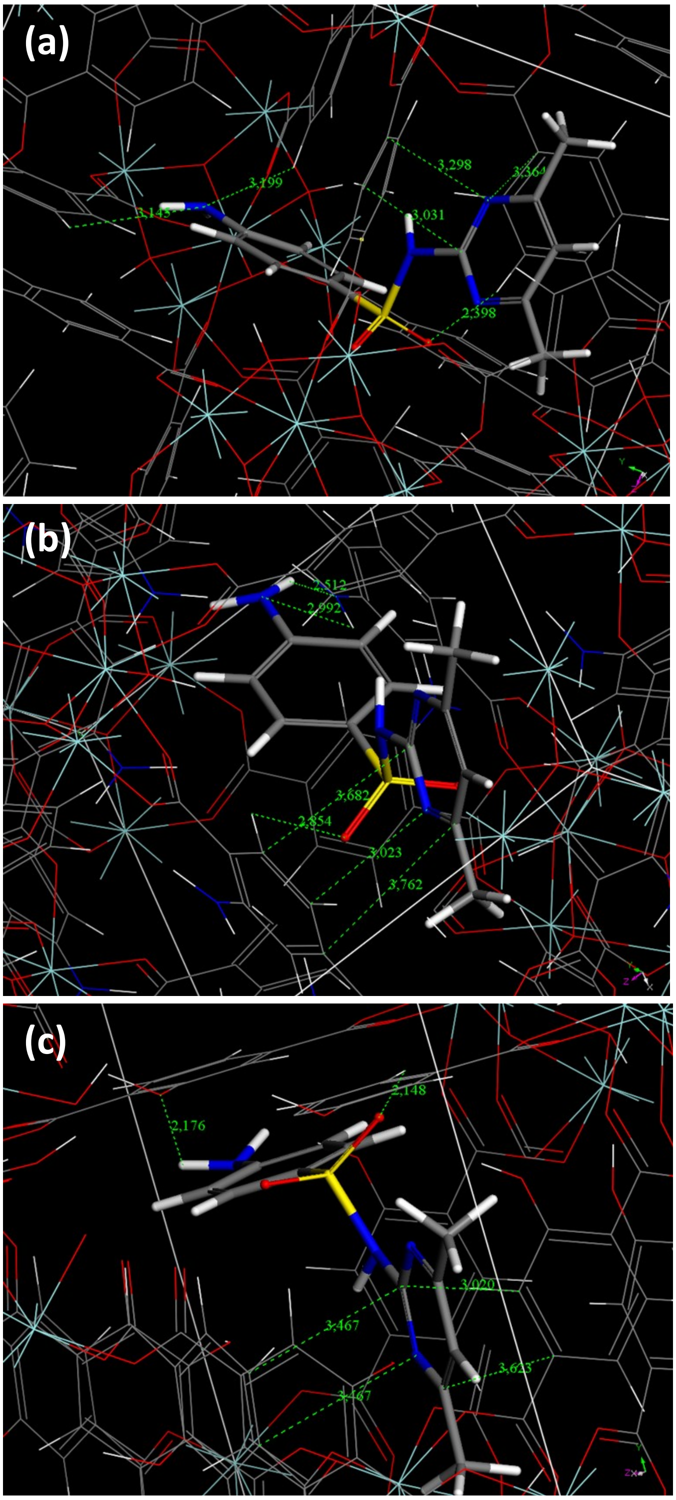

Figure S9. Main interactions observed on snapshots extracted from Monte Carlo simulations (loading fixed at 1 molecule of SMT/u.c.) for UiO-66-X (X= H (a), NH_2 (b), and OH (c)).

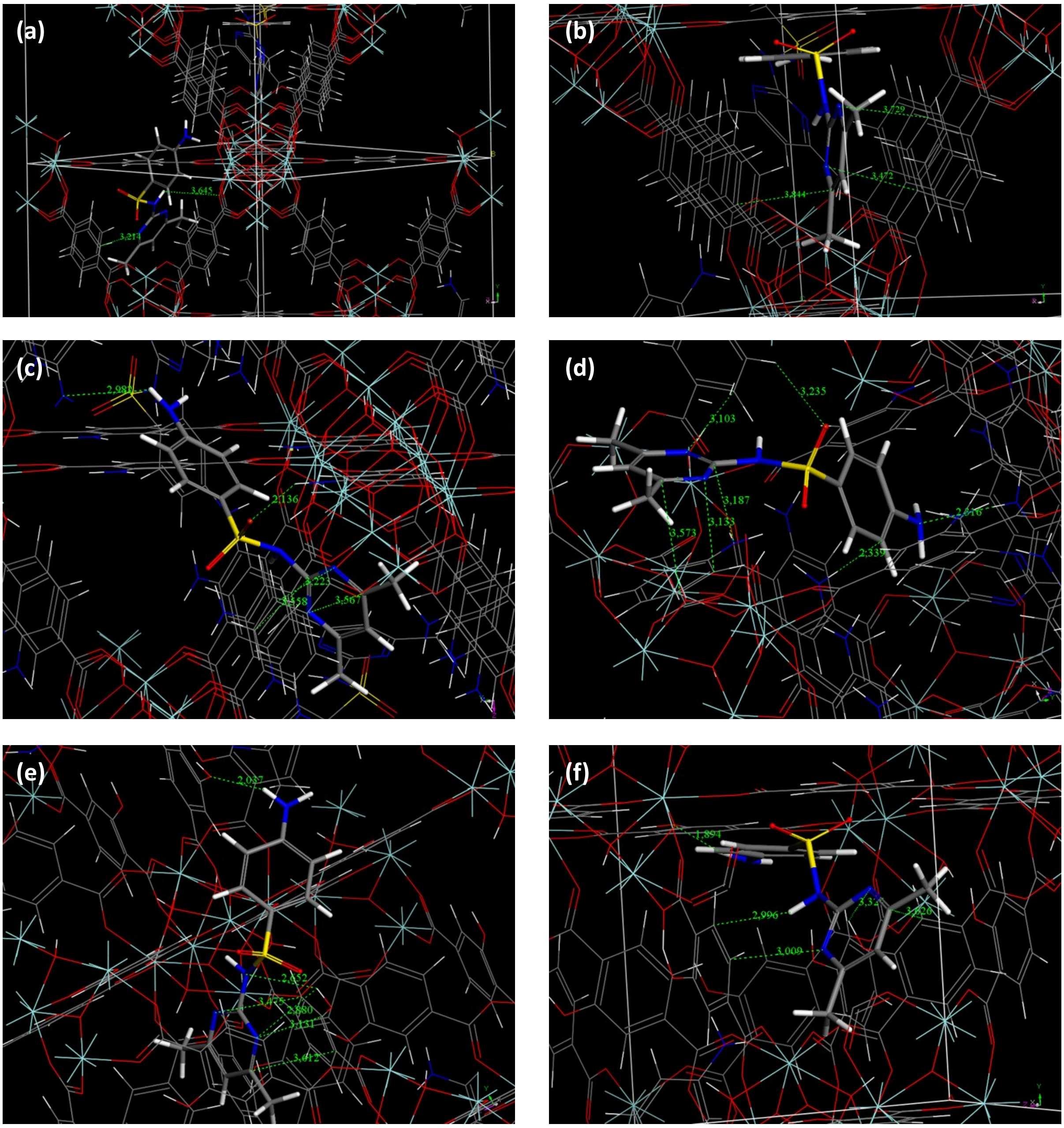

Figure S10. Main interactions observed on snapshots extracted from DFT calculations for UiO-66-X in tetrahedral and octahedral cages, respectively (X= H (a) and (b); NH_2 (c) and (d); and OH (e) and (f)).

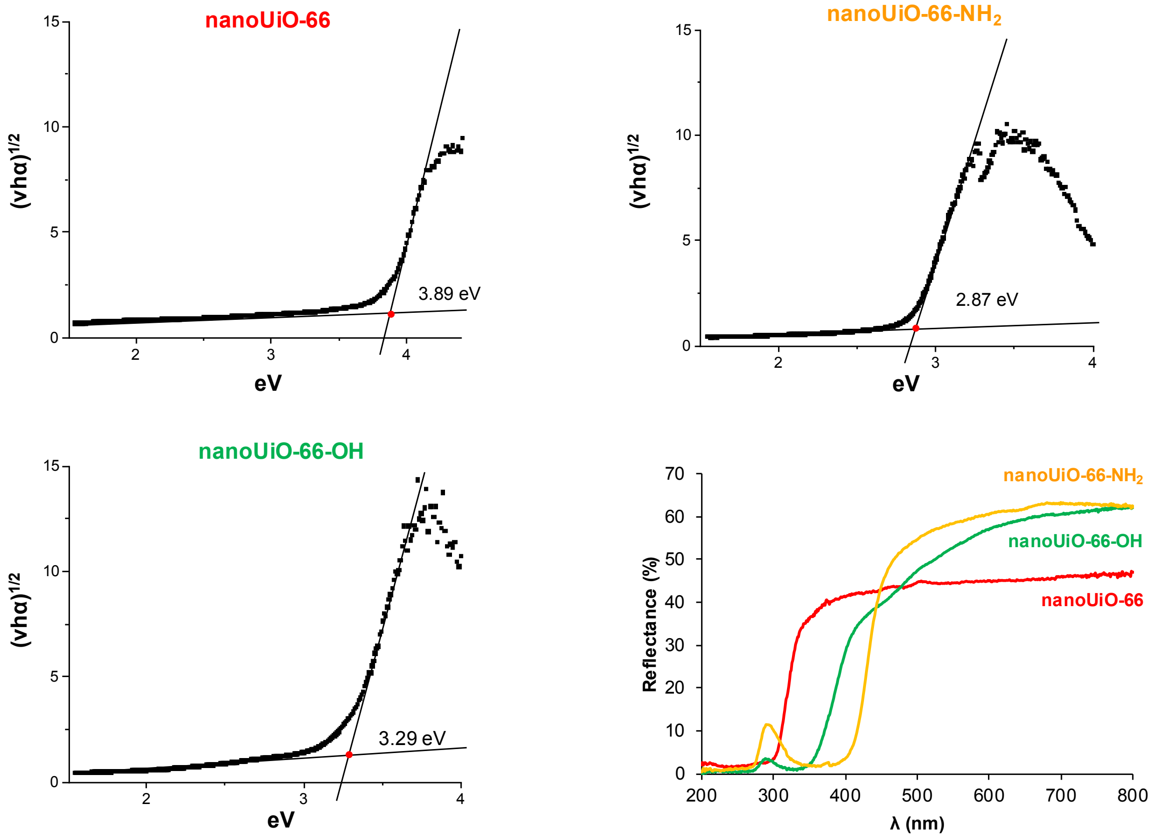

Figure S11. Band gap estimated from the Tauc plot,[1] and diffuse reflectance analysis of UiO-66-X (X = H, NH_2, OH).

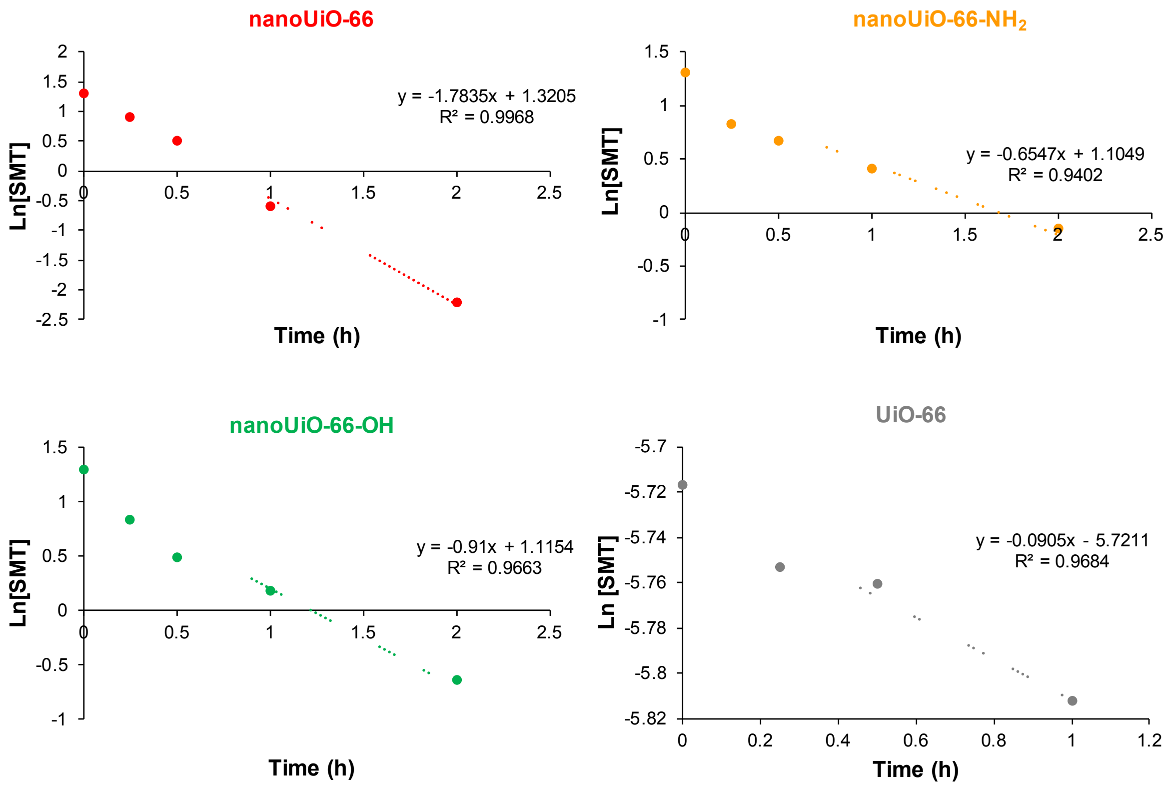

Figure S12. Fitting of SMT degradation data using nanoUiO-66-X (X = H, NH_2, and OH) and UiO-66 to a first order kinetics.

Table S3. Comparison of degraded SMT values (% and $mg·L^{-1}·min^{-1}$) using nanoUiO-66-X, UiO-66 and other MOF-based catalysts, as well as ZnO and TiO_2.

MOF based material	**SMT degraded (%)**	**Time (min)**	**Kinetic model**	***K***	**Refs**
UiO-66	35	240	1st	0.0905 ± 0.039 h^{-1}	This work
nanoUiO-66	100	240	1st	1.7835 ± 0.0587 h^{-1}	This work
nanoUiO-66-NH_2	91	240	1st	0.6547 ± 0.0953 h^{-1}	This work
nanoUiO-66-OH	95	240	1st	0.91 ± 0.098 h^{-1}	This work
CUS@MIL-100(Fe)	100	180	ND	ND	2
PW_{12}@MFM-300(In)	98	120	ND	ND	3
MIL-53(Fe)@percarbonate	90	60	ND	ND	4
ZnO/glass plate	96	300	pseudo-2nd	0.002 $L·mg^{-1}$ min^{-1}	5
TiO_2	95	120	ND	ND	6

ND: no data reported

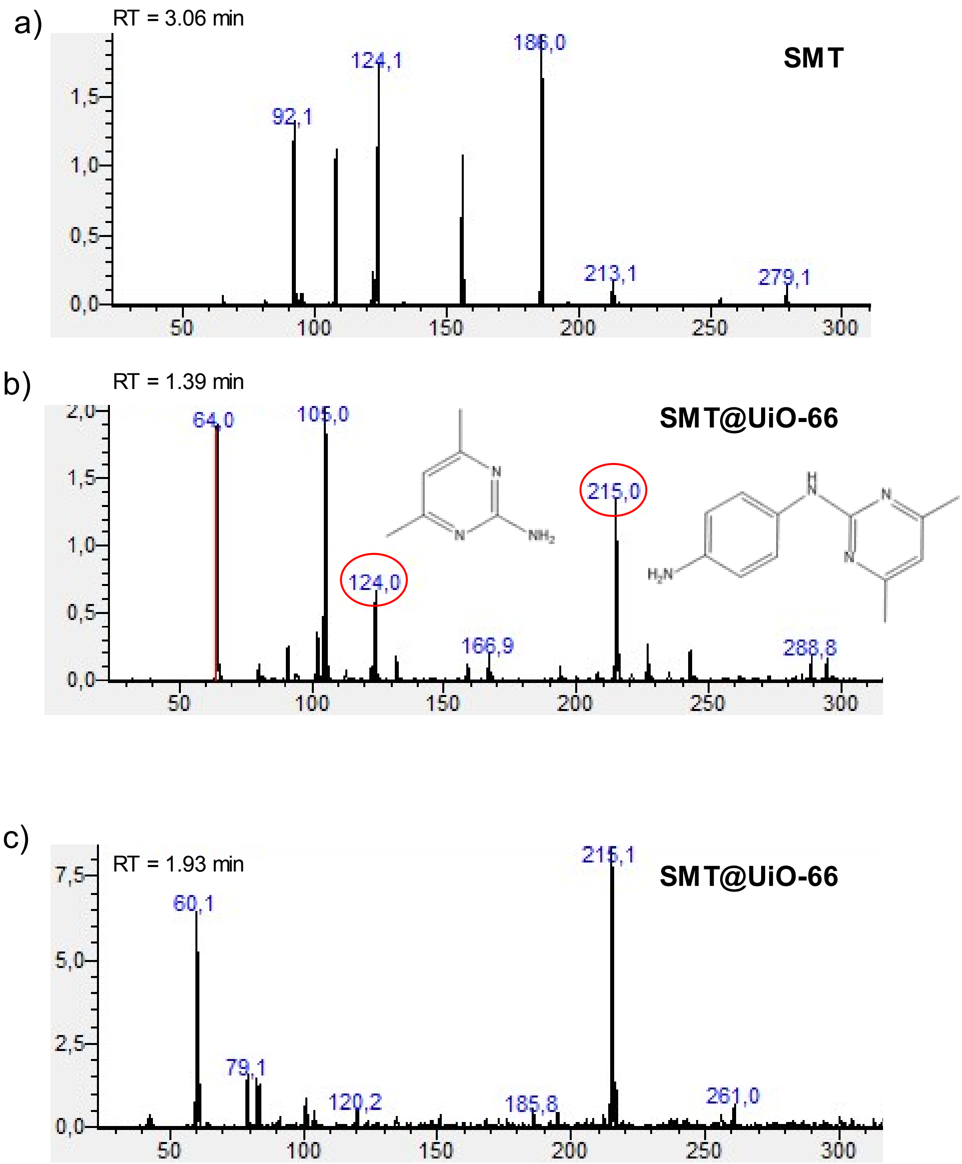

Figure S13. MS spectra of the intermediates detected in the photocatalytic degradation of a) SMT, and b) and c) SMT in the presence of UiO-66 under UV-vis light irradiation.

S4. References

1 B. D. Viezbicke, S. Patel, B. E. Davis and D. P. Birnie, *Phys. status solidi*, 2015, **252**, 1700–1710.

2 J. Tang and J. Wang, *Environ. Sci. Technol.*, 2018, **52**, 5367–5377.

3 G. Li, K. Zhang, C. Li, R. Gao, Y. Cheng, L. Hou and Y. Wang, *Appl. Catal. B Environ.*, 2019, **245**, 753–759.

4 R. Li, Z. Chen, M. Cai, J. Huang, P. Chen and G. Liu, *Appl. Surf. Sci.*, 2018, **457**, 726–734.

5 T. Aissani, I. Yahiaoui, F. Boudrahem, L. Yahia Cherif, F. Fourcad, A. Amrane and F. Aissani-Benissad, *React. Kinet. Mech. Catal.*, 2020, **131**, 481–487.

6 S. Fukahori and T. Fujiwara, *J. Environ. Manage.*, 2015, **157**, 103–110.